Deep-Sea Research I 55 (2008) 1474–1483

Contents lists available at ScienceDirect

Deep-Sea Research I

journal homepage: www.elsevier.com/locate/dsri

The potential influence of bioluminescence from marine animals on a deep-sea underwater neutrino telescope array in the Mediterranean Sea

Imants G. Priede [a,*], Alan Jamieson [a], Amandine Heger [a], Jessica Craig [a], Alain F. Zuur [b]

[a] Oceanlab, University of Aberdeen, Main Street, Newburgh, Aberdeen AB41 6AA, UK[1]
[b] Highland Statistics Ltd., 6 Laverock Road, Newburgh AB41 6FN, UK

ARTICLE INFO

Article history:
Received 15 March 2008
Received in revised form
28 June 2008
Accepted 3 July 2008
Available online 5 July 2008

Keywords:
Bioluminescence
Neutrino telescope
Mediterranean Sea
KM3NeT

ABSTRACT

The density of bioluminescent organisms in the water column was measured using a vertically descending impact screen technique at experimental underwater neutrino telescope sites in the Eastern Mediterranean (Ionian Sea NESTOR 36°37′N 21°21′E) and in the Western Mediterranean Sea (Ligurian Sea ANTARES 42°25′N 6°11′E). The mean density at depths >1500 m in the Ligurian Sea was 0.622 m^{-3} and at 1500–2500 m in the Ionian Sea it was 0.068 m^{-3}. At greater depths in the Ionian Sea, density decreased to 0.043 m^{-3} at 2500–3500 m and 0.018 m^{-3} at >3500 m. At these densities it is predicted that the effect of natural background bioluminescence would be negligible in its effect on the telescope. Modelling encounter of bioluminescent organisms carried in deep-sea currents impinging on a telescope photo-detector predicts bioluminescent flashes, 16.59 h^{-1} at ANTARES and at NESTOR 1.84 h^{-1} at 1500–2500 m depth, 1.16 h^{-1} at 2500–3500 m and 0.49 h^{-1} at >3500 m.

1. Introduction

A new human activity in the deep-sea is the construction of undersea neutrino telescopes for detecting neutrinos originating from cosmic sources both within the local galaxy and from extragalactic sources (Carr and Hallewell, 2004). Neutrinos passing through matter decay into muons, which in turn stimulate emission of Čerenkov light in sea water. Neutrino telescopes are based on using a three-dimensional array of photo-detectors within a large volume of water. Timing the arrival of Čerenkov photons at different elements of the array allows determination of muon trajectory and hence tracing of parent neutrinos back to their cosmic origin. The telescope is designed to mainly detect upward-directed muons generated by interactions of neutrinos that have passed through the earth from the antipodes. The major pioneering project of this kind was DUMAND (Deep Underwater Muon and Neutrino detector), which began work off the coast of Hawaii in 1980 with detectors linked to underwater cables (Babson et al., 1990). The technical difficulties were immense and the project was abandoned in 1995. However, following advances in underwater technology there is now renewed interest with three experiments in the Mediterranean Sea (Fig. 1); NESTOR at 4100 m depth off the coast of Greece (Anassontzis and Koske, 2003) achieved the first reconstructions of muon tracks in 2003 (Aggouras et al., 2005a, b). ANTARES off the south coast of France at 2500 m began operation of a prototype detector in 2005 (Aguilar et al., 2006; Stolarczyk et al., 2007), and the complete 0.1 km^2 telescope array comprising 12 strings was completed in May 2008. NEMO in the Ionian Sea east of Sicily deployed a cable for a stage 1 experiment in 2005 at 2000 m depth and have defined a

* Corresponding author. Tel.: +44 1224 274408; fax: +44 1224 274402.
E-mail address: i.g.priede@abdn.ac.uk (I.G. Priede).
[1] A participating institute in the KM3NeT consortium: http://www.km3net.org.

0967-0637/$ - see front matter © 2008 Elsevier Ltd. All rights reserved.
doi:10.1016/j.dsr.2008.07.001

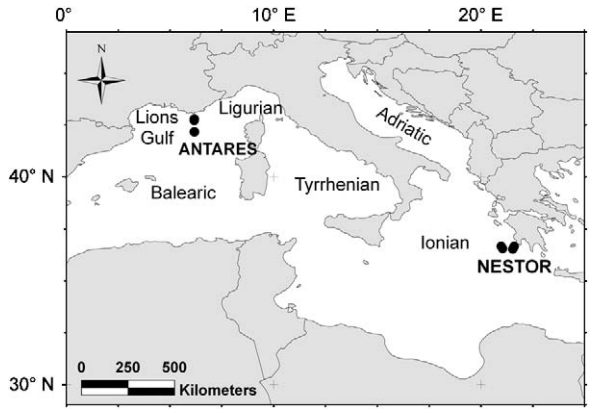

Fig. 1. Chart of the Mediterranean Sea showing the location of the ANTARES and NESTOR neutrino telescope sites.

site at 3500 m depth (Margiotta et al., 2006). A European collaboration (KM3NeT) is undertaking a design study for a 1 km^3 detector to be built in the Mediterranean Sea (Katz, 2006).

In addition to light from high-energy neutrino-derived muons, undersea neutrino telescopes detect photons produced by the radioactive decay of dissolved potassium-40 (^{40}K) in seawater, and bioluminescence. Bioluminescence in the deep-sea is generally blue, centred on the wavelength of maximum transmissivity of sea water (480 nm) and is of two kinds, bioluminescence from free-living bacteria that contributes to a steady low-level background light and non-steady-state flashes produced by deep-sea animals. A deep-sea location is required for neutrino telescopes for a number of reasons:

(a) Depth must be greater than the maximum depth of penetration of solar light.
(b) Deep water is necessary to accommodate the dimensions of the array that may be up to 1000 m high.
(c) High transparency and optimal optical properties of deep-sea water.
(d) Need for shielding from downward background muons originating in the atmosphere.
(e) Low levels of bioluminescence.
(f) Low rates of biofouling on the array structure and optical surfaces.
(g) Generally low water current velocity to avoid distortion of the array and stimulation of bioluminescence.

In the deep sea, bioluminescent flashes from animals are likely to produce the highest photon counts observed and may limit the performance of the telescope. In the presence of bioluminescence, nearby detectors are saturated and are unable to detect Čerenkov photons. Whilst bioluminescence cannot be mistaken for Čerenkov photons the probability of detection of rare cosmic events such as super-novas is reduced. Measurements associated with the DUMAND experiment in the Pacific Ocean off Hawaii indicated that the number of bioluminescence events decreases exponentially with depth and instruments above the sea floor at depths greater than 3000 m detected "giant flashes" at frequencies of 2–5 h^{-1} (Bradner et al., 1987; Webster et al., 1991). However, these flashes may have been stimulated by motion of the measuring instrument relative to the surrounding water. Observations from manned submersibles passively floating in mid-water, albeit at shallower depths (Widder et al., 1989), indicate that the frequency of natural background bioluminescence is much lower than those recorded by optical instruments either moving or suspended in the water column.

In this paper, we measure the abundance of bioluminescent organisms in the water column at two of the experimental neutrino telescope sites in the Mediterranean Sea and make predictions of the number of luminescent flashes occurring at a typical detector element of a neutrino telescope. Most deep-sea animals are capable of producing light but since this requires energy, emissions are produced sparingly and occur most notably in emergency situations. We assume that bioluminescent planktonic animals exhibit an alarm response on contact with, or proximity to solid surfaces and respond by a flash of light or emission of luminescent fluid into the surrounding medium. This is intended to act as a deterrent or distraction to a potential predator and is likely to be the main source of animal luminescence affecting the neutrino telescope infrastructure.

2. Methods

2.1. Measurement of density of bioluminescent animals

The density (number m^{-3}) of animals with luminescent capability was measured by traversing a mesh screen through the water and observing stimulated luminescence as animals impact on, or pass through the mesh. This technique, first developed by Widder et al. (1989) for horizontal profiling, was adapted to vertical profiling by Priede et al. (2006). The stimulated luminescence was recorded using a high sensitivity ISIT video camera (OE1325: Kongsberg Simrad, UK, faceplate sensitivity 5×10^{-6} lx or $-4\log^{10}$ mW m^2 at 1 m at $\lambda=470$ nm) recording onto a DV tape recorder (GV-D300; Sony, Japan), controlled via a custom-built programmable logging system (Priede et al., 2006). Incorporating a battery pack, this was an autonomous system that could be mounted on a free-fall vehicle (Priede et al., 2006) or lowered by wire on a CTD frame (Heger et al., 2008). The camera was focused looking downwards at the mesh screen (dimensions 0.38×0.5 m and mesh pitch 8×16 mm) which was placed in the horizontal plane, and the whole system descended through the water column at constant speed. The number of events, each corresponding to the presence of an animal, was counted during replay of the recording in the laboratory. Knowing the area of the mesh screen and descent velocity, the abundance of luminescent animals was readily calculated.

Studies were done during four expeditions to the Mediterranean Sea (Fig. 1). The ANTARES site in the

Table 1
Details of bioluminescence profiles

ID	Name	Date	Latitude	Longitude	Bottom depth (m)
AJ2	ANTARES inshore	23 January 2004	42°48.00′N	6°10.70′E	2494
AM2	ANTARES inshore	18 May 2004	42°10.51′N	6°10.70′E	2494
AM3	ANTARES Intermediate	18 May 2004	42°44.00′N	6°10.70′E	2442
AJ5	ANTARES offshore	24 January 2004	42°10.51′N	6°10.70′E	2479
AM5	ANTARES offshore	19 May 2004	42°10.51′N	6°10.70′E	2479
N5.2	NESTOR 5.2	16 October 2006	36°33.61′N	21°02.79′E	4957
N4.5	NESTOR 4.5	16 May 2007	36°32.16′N	21°28.12′E	4480
N6	NESTOR 6	16 May 2007	36°40.58′N	20°59.01′E	3955
N3	NESTOR 3	17 May 2007	36°37.28′N	21°34.08′E	3829
N2	NESTOR 2	18 May 2007	36°40.52′N	21°39.61′E	2200

Ligurian Sea was visited in January and May 2004 on board the GGIX fast catamaran. The free-fall technique was used since this vessel was too small for an oceanographic winch with an appropriate length of cable. Profiles were done at the ANTARES site 20.5 km south of Île de Porquerolles, Hyères, an intermediate site 7.4 km further south and an offshore location 90 km from Île de Porquerolles.

The NESTOR site in the Ionian Sea was visited on board the F.S. *Meteor* (Cruise M70/1) in October 2006 and on board the R.V. *Aegaeo* in May 2007 with the bioluminescence profiler fitted onto the ship's CTD rosette frame. Five locations were investigated from 26 to 68 km offshore (Table 1).

The free-fall lander used at the ANTARES site in the Ligurian Sea descended at $0.25\,m\,s^{-1}$ whereas at the NESTOR site in the Ionian Sea the CTD frame was lowered at $0.8\,m\,s^{-1}$. These velocities are well above the $9\,mm\,s^{-1}$ threshold necessary to generate sufficient shear forces to stimulate bioluminescence as animals pass through the mesh (Priede et al., 2006). For analysis of the data, counts were made of number of bioluminescent events in volumes of water (V) corresponding to 90 s descent time increments in the Ligurian Sea and 60 s for the Ionian Sea.

To analyse the abundance of bioluminescent organisms, and determine whether there are significant differences between profiles, a generalised additive model (GAM; Wood, 2006) with a Poisson distribution was used. The bioluminescent data were measured as a density, but to take account of sampling different water volume increments (V) it was assumed that:

$$BL_{ij} \sim \text{Poisson}(\mu_{ij} \times V_{ij}),$$

where BL_{ij} is the observed bioluminescence in profile i at depth j, $\mu_{ij} \times V_{ij}$ is the expected value, and V_{ij} is the intensity parameter of the Poisson distribution. The Poisson distribution dictates that the mean equals the variance: $E(BL_{ij}) = \text{Var}(BL_{ij}) = \mu_{ij}V_{ij}$. Using the log-link function in the GAM gives the following model:

$$\mu_{ij} \sim e^{\alpha_i + \log(V_{ij}) + s(\text{Depth}_{ij})}. \quad (1A)$$

The differences in water volumes enters the model as an offset variable, which means that there is no regression parameter in front of the term $\log(V_{ij})$. The notation $s(\text{Depth}_{ij})$ stands for smoothing function, which is typically estimated with a smoothing spline. To make the smoother unique, it is centred at 0. The amount of smoothing was estimated with cross-validation (Wood, 2006; Zuur et al., 2007).

The GAM in Eq. (1A) uses a different intercept for each profile, and the same smoother for each profile. The intercepts are not strictly intercepts as we know them from linear regression. Instead, they can be seen as a type of average of the abundances per profile, after taking into account the depth (and volume) effect.

There are a series of possible model improvements. Gillibrand et al. (2007) used random effects to replace the 10 intercepts. However, in this case, we were particular interested to know whether intercepts from the NESTOR and ANTARES profiles are different from each other. Hence, we also applied a model of the form:

$$\mu_{ij} \sim e^{\alpha_k + \log(V_{ij}) + s(\text{Depth}_{ij})}. \quad (1B)$$

The index k is 1 for profiles from ANTARES and 2 for profiles from NESTOR. Another model extension we applied was related to the smoothing functions. In Eqs. (1A) and (1B) we used 1 smoother for all 10 profiles, implying that the depth–abundance relationship is the same at each profile. A first potential improvement is to use a model with two smoothers, one for the ANTARES profiles, and one for the NESTOR profiles:

$$\mu_{ij} \sim e^{\alpha_i + \log(V_{ij}) + \sum_k s_k(\text{Depth}_{ij})}. \quad (2A)$$

The index k again discriminates between the two areas. It is also possible to use a model with two smoothers, and two intercepts. This would be the (1B) equivalent of (2A). The final set of models we considered contained 10 smoothers; one for each profile:

$$\mu_{ij} \sim e^{\alpha_i + \log(V_{ij}) + \sum_i s_i(\text{Depth}_{ij})}. \quad (3A)$$

Again, we have the choice between 10 intercepts or 2 (one for each area), which is model 3B.

Comparing these models, for example 1A versus 1B, 2A versus 2B or 3A versus 3B gives us the tools to judge whether the five profiles per area have the same mean value, or not. By comparing 1A, 2A and 3A, we know whether the 10 profiles have the same depth–abundance pattern, whether it differs per area, or whether all patterns are different. The same can be done for 1B, 2B and 3B.

It is also possible to use models with, for example one smoother for the NESTOR profiles and two smoothers for the ANTARES profiles. However, because the underlying question of this study is whether there are any differences between the profiles of the two areas, we only focus on models 1, 2 and 3.

To find the optimal model, the Akaike Information Criterion (AIC) was used. None of the models contained overdispersion. A model validation was applied on the optimal model, and we looked at independence of Pearson residuals within a series, and between the series. Once, the optimal model is found, the abundance can easily be transformed to densities by dividing the expected value μ_{ij} by V_{ij}.

2.2. Prediction of frequency of bioluminescent events

The deep-sea neutrino telescope is likely to detect three kinds of pelagic bioluminescence from animals: spontaneous, stimulated and entrained. Spontaneous or "natural" bioluminescence describes events that occur in the absence of external stimuli. The dominant effect is likely to be events stimulated by impact of organisms or their appendages with a photo-detector sphere or part of the array structure. Entrainment can occur if, for example the tentacles of a jelly-fish become entangled with the structure which will result in repeated flashes of light following the initial impact.

The probability of bioluminescent organisms impinging on a stationary object such as a spherical optical module (OM) can be modelled as a function of the sphere diameter, ϕ_{sphere}, the animal diameter, ϕ_{animal}, the density, ρ (bioluminescent sources m^{-3}), and the current velocity, v, and yields the expression:

$$\text{Impacts } s^{-1} = \pi\left(\frac{\phi_{\text{sphere}}}{2}+\frac{\phi_{\text{animal}}}{2}\right)^2 \times v \times \rho, \quad (4)$$

where v is the current velocity ($m\,s^{-1}$) and ρ is the density (number of sources m^{-3}).

It is assumed that each impact will result in at least one flash from a luminescent organism. It is unlikely that stimulation will be the result of direct impact of the animal on the sphere, since most planktonic animals have sensory organs that can detect proximity of objects and most likely respond when shear forces in the flow around the sphere exceed a threshold level as described by Hartline et al. (1999). Most of the light output is likely to occur downstream of the OM owing to: time delay between stimulation and light output, development of highest stimulatory forces in vortices downstream of the OM, entrainment of organisms in the downstream vortices and mutual stimulation as these animals respond to one another.

Buskey and Swift (1990) proposed that natural occurrence of bioluminescent flashes could be predicted by the relationship:

$$\text{Encounters } s^{-1} = \frac{\pi R^2 \rho}{3}\frac{u^2+3v^2}{v}, \quad (5)$$

where R is the encounter radius defined by the bioluminescent animal's sensory system, ρ the density of other plankton, v the swimming velocity of the bioluminescent animal and u is the swimming velocity of other plankton. They assumed that whenever a bioluminescent organism meets a non-luminescent zooplankter this would be marked by a bioluminescent event. This model ignores possible flashes resulting from mutual interactions between bioluminescent zooplankters. For the purposes of calculation we assume that ρ is 10 times the density of bioluminescent sources as measured by our profiler.

2.3. Magnitude of bioluminescent events

Bioluminescent organisms can be grouped into three size categories following the generally accepted size classification of marine plankton (Dussart et al., 1965; Sieburth et al., 1978): mesoplankton (0.2–20 mm) consisting mainly of small crustaceans (e.g. copepods), macroplankton (20–200 mm) including principally large pelagic crustaceans (e.g. euphausiids), and megaplankton (200–2000 mm) encompassing mostly gelatinous zooplankton from single individuals (e.g. medusae) to large colonial organisms (e.g. siphonophores, pyrosomes).

There are a number of reports in the literature quantifying light output from marine organisms stimulated in various ways. We have reviewed these data (Heger, 2007) and for purposes of comparison converted those with sufficient information to total number of photons per flash emitted over an entire sphere of 4π steradians with the organism at the centre.

3. Results

In all the profiles, there was a decrease in density of bioluminescent sources with depth down to ca. 1000–1500 m followed by relatively constant values in deeper water (Fig. 2). Counts were not possible near the surface in daylight and recording was generally not started until depths of interest to neutrino telescopes had been reached.

Fitted curves from generalised additive modelling are superimposed on the data in Fig. 3. The AIC values for the six GAMs are given in Table 2. Models 1A and 1B are nested, and instead of using the AIC to judge which model is better, we also applied a likelihood ratio test. This gave $\chi^2 = 262.36$, $df = 7.00$, $p < 0.001$ indicating that the model with 10 intercepts and one smoother was significantly better than a model with two intercepts and one smoother. In model 2A we used two smoothers (one per area) and 10 intercepts, whereas in model 2B two smoothers and two intercepts (one per area). The AIC indicated that 2A was better than 2B. The same held for models 3A and 3B; 3A was better. These results indicated that all 10 profiles have different mean values.

Comparing the AICs of models 1A and 2A indicated that a model with two smoothers (one per area), is better than a model with only one smoother for both areas. This is also confirmed by a likelihood ratio test ($\chi^2 = 18.44$, $df = 3.62$, $p < 0.001$). Model 3A used 10 different smoothers, one for each profile, $s(\text{Depth}_{ij})$ and was better (as judged by the AIC) than all other models with each

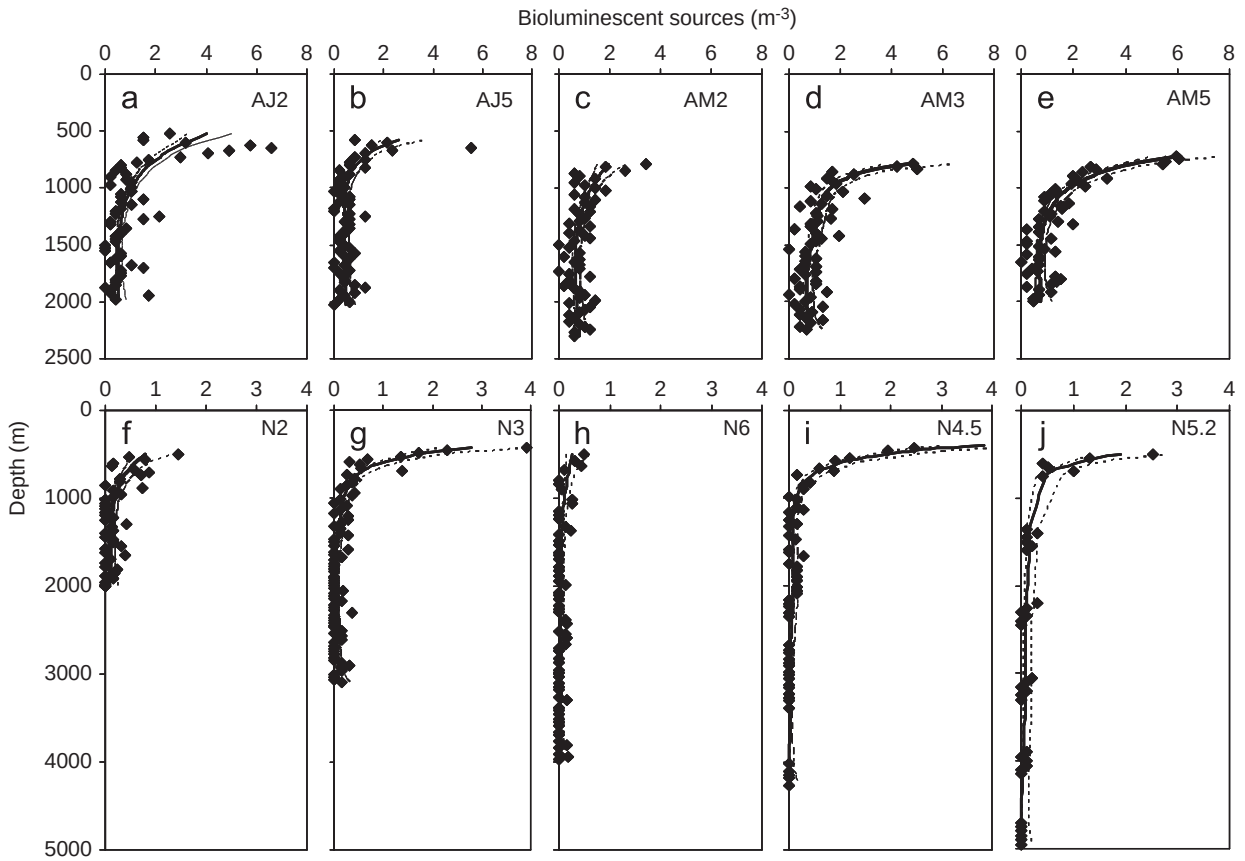

Fig. 2. Scatter plots of density of bioluminescent sources as a function of depth in the Eastern and Western Mediterranean Sea. Upper row (a)–(e), Western Mediterranean, Ligurian Sea ANTARES locations. Lower row (f)–(j) Eastern Mediterranean, Ionian Sea NESTOR locations. Note the difference in the density scale (m^{-3}) between the upper and lower rows. Each point corresponds to a count of flashes detected by the profiler converted to number m^{-3}. (a) and (b) January 2004. (c)–(e) May 2004. Keys to stations are as in Table 1. Superimposed are fitted curves derived from GAMS, solid line—predicted value. Dashed lines—upper a lower 95% confidence limits.

profile having a different intercept α_i 80.2% of the deviance was explained and $p<0.001$. These are the curves shown in Fig. 3. In Fig. 3 it is evident that the predicted abundance of bioluminescent organisms at all depths is higher in the Ligurian Sea than in the Ionian Sea. Table 3 compares the mean values in the different profiles, the overall average over the depth range from 1500 to 2500 m or maximum depth of the profile was almost 10 10-fold higher in the Ligurian Sea than the Ionian. The respective maximum values observed were 1.71 and 0.39 m^{-3}.

No consistent trend of change in abundance with distance offshore could be discerned at either site. Furthermore although seasonal changes were evident at ANTARES site between January and May the effect was different offshore and inshore. At depths over 4000 m at the NESTOR site no sources were detected at N4.5 and 0.011 m^{-3} at N5.2. The gaps in the data for these two stations (Fig. 2) correspond to times when the instrument was switched off to distribute the available 1 h recording capacity of the Digital Video Tape over the whole depth of the profile.

Table 4 shows the predicted frequencies of bioluminescent flashes at a photo-detector resulting from different densities of bioluminescent organisms. Calculations were done for a sphere of 432 mm diameter similar to the widely used standard 17 in. glass sphere (Teledyne Benthos, North Falmouth, MA, USA). The background was calculated for a 1 m^3 of water and a volume equal to 10 m radius. Interactions of organisms with the photodetector are likely to be much more important than the predicted natural background.

Magnitudes of bioluminescent events are listed in Table 5 and are reproduced visually in Fig. 4. Generally the flashes vary between 10^{10} and 10^{12} photons emitted over a duration of 1–15 s. The ability to repeat flashes varies considerably from small copepods, which might exhaust all their potential within a few flashes, to jellyfishes (scyphozoa) and the large colonial organisms (siphonophores and pyrosomes) that can continue repeat flashing for many hours.

4. Discussion

The abundance of deep-sea bioluminescent organisms in the Mediterranean Sea is much lower than at equivalent

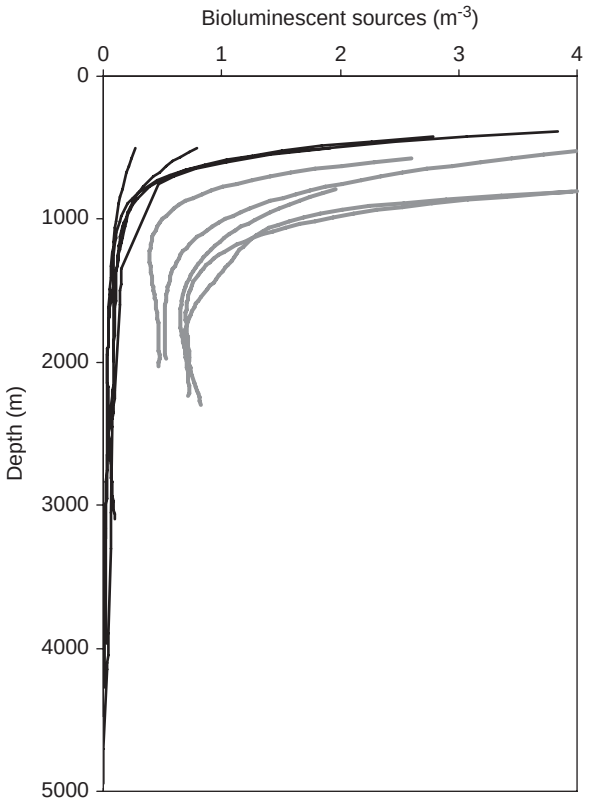

Fig. 3. Predicted density of bioluminescent sources as a function of depth in the Eastern and Western Mediterranean Sea from generalised additive modelling. Black lines—Eastern Mediterranean, Ionian Sea, NESTOR sites. Grey lines—Western Mediterranean Sea, Ligurian Sea, ANTARES sites.

Table 2
AIC values of various models

Model	Equation	AIC
1A	$\mu_{ij} \sim e^{\alpha_i + \log(V_{ij}) + s(\mathrm{Depth}_{ij})}$	2022.876
1B	$\mu_{ij} \sim e^{\alpha_k + \log(V_{ij}) + s(\mathrm{Depth}_{ij})}$	2271.199
2A	$\mu_{ij} \sim e^{\alpha_i + \log(V_{ij}) + \sum_k s_k(\mathrm{Depth}_{ij})}$	2011.684
2B	$\mu_{ij} \sim e^{\alpha_k + \log(V_{ij}) + \sum_k s_k(\mathrm{Depth}_{ij})}$	2202.272
3A	$\mu_{ij} \sim e^{\alpha_i + \log(V_{ij}) + \sum_i s_i(\mathrm{Depth}_{ij})}$	1997.747
3B	$\mu_{ij} \sim e^{\alpha_k + \log(V_{ij}) + \sum_i s_i(\mathrm{Depth}_{ij})}$	2002.325

The lower the AIC, the better the model. In models 1A and 1B, one smoother is used for all 10 profiles. In 1A, we used 10 intercepts, and in 1B one intercept per area (ANTARES versus NESTOR). In models 2A and 2B, two smoothers are used, one for the ANTARES profiles, and one for the NESTOR profiles. In 2A, we use 10 intercepts, and in 2B only two (one per area). Model 3A uses 10 smoothers, and 10 intercept allowing for a different mean value per profile. In 3B, 10 smoothers and two intercepts are used.

depths previously investigated in the Atlantic Ocean and it is demonstrated that there is a clear benefit in terms of reduction of probable bioluminescent interference in locating the KM3NeT array in the Mediterranean Sea. Furthermore values in the Ionian Sea are an order of

Table 3
Mean values of density of bioluminescent sources (number m^{-3}) over different depth ranges in the Ligurian Sea and the Ionian Sea compared with corresponding data from the NE Atlantic Ocean (Gillibrand et al., 2007)

	Depth range		
	1500–2500 m	2500–3500 m	>3500 m
Ligurian Sea (ANTARES)			
AJ2	0.512	–	–
AJ5	0.465	–	–
AM2	0.708	–	–
AM3	0.731	–	–
AM5	0.696	–	–
Mean	0.622	–	–
Ionian Sea (NESTOR)			
N2	0.091	–	–
N3	0.037	0.075	–
N6	0.025	0.031	0.030
N4.5	0.084	0.000	0.000
N5.2	0.101	0.067	0.025
Mean	0.068	0.043	0.018
NE Atlantic			
Spring	3.075	1.554	0.466
Autumn	11.813	1.640	0.593

magnitude lower than in the Ligurian Sea. These measurements should be treated with caution because there can be considerable spatial and temporal patchiness in abundance of bioluminescent organisms. For example Widder et al. (1999) found dense aggregations of the bioluminescent copepod *Metridia lucens* in thin layers less than 0.5 m thick at density discontinuities between the surface and 200 m depth in the Gulf of Maine extending horizontally over 72 m. In the temperate NE Atlantic Ocean west of Ireland, Gillibrand et al. (2007) found a strong seasonal effect with a thick layer of over 25 bioluminescent organisms m^{-3} developing from August of each year at 1500 m depth compared with 6 m^{-3} at the same depth in spring. It can be assumed that the abundance of bioluminescent organisms at depth is a function of productivity in the overlying waters from which organic matter is exported downwards by sedimentation of particulate organic matter. In the NE Atlantic there is an annual peak of surface primary production in May coinciding with surface chlorophyll concentrations of ca. 3 mg m^{-3} (Lampitt et al., 2001) implying a delay of 2–3 months between surface production and increase in bioluminescence organisms at 1500 m. In the Mediterranean Sea, chlorophyll concentrations are typically in the range 0.1–1 mg^{-3} (Bricaud et al., 2002) so our observations of bioluminescence at depth are in accord with the general evidence that the Mediterranean Sea is characterised by low biological productivity decreasing towards the east. In the Mediterranean Sea the peak of surface chlorophyll concentration is in winter (January–February) but peak production is in June and July when

Table 4
Predicted number of bioluminescent flashes in the vicinity of a detector at the ANTARES and NESTOR locations in the Mediterranean Sea

	Density (m^{-3})	Impacts on detector		Background		
		Flash rate		Flash interval (min)		
		min^{-1}	h^{-1}		($1\,m^3$)	$r = 1$ m
ANTARES 1500–2500 m	0.622	0.28	16.79	3.57	2.29×10^4	5.46×10^3
NESTOR 1500–2500 m	0.068	0.031	1.84	32.69	1.91×10^6	4.57×10^5
NESTOR 2500–3500 m	0.043	0.019	1.16	52.68	4.78×10^6	1.14×10^6
NESTOR >3500 m	0.018	0.008	0.49	125.47	2.73×10^7	6.51×10^6

Densities of bioluminescent plankton are means taken from Table 3. For flashes stimulated by direct impact on a spherical photo-detector a water velocity of 0.05 m s^{-1} is assumed and an effective animal diameter of 5 mm. Background flash intervals are calculated for water volumes of 1 m^3 and 1 m radius with a plankton encounter radius of 3 mm, swimming speed of 5 mm s^{-1} and 10:1 ratio of abundance of non-bioluminescent to bioluminescent plankton (Buskey and Swift, 1990).

Table 5
Total quantum emission of individual flashes by different marine bioluminescent organisms in response to a single stimulus (mean values)

Group	Species	Mean total quantum emission (photons $flash^{-1}$)	Intensity (W m^{-2} at 1 m)	Wavelength (nm)	Duration (s)	Mode of stimulation	References
Copepoda	*Gaussia princeps*	1.8×10^{11}				Electrical	Bowlby and Case (1991)
	Pleuromamma xiphias	1.8×10^{10}				Mechanical	Latz et al. (1990)
	Metridia lucens	1.7×10^9	0.02×10^{-9}	480		Electrical	Clarke et al. (1962)
	Metridia lucens	6.6×10^{12}	32.4×10^{-9}	480		Mechanical	Clarke et al. (1962)
Euphausiiacea	*Meganictyphanes norvegica*	1.2×10^{11}	0.3×10^{-9}	475		Electrical	Clarke et al. (1962)
	Euphausia eximia	1×10^{10}				Vacuum	Lapota and Losee (1984)
	Nyctiphanes simplex	1×10^{11}				Vacuum	Lapota and Losee (1984)
Amphipoda	*Cyphocaris faurei*	5.7×10^{10}				Mechanical	Bowlby et al. (1991)
	Scina crassicornis	3.1×10^{10}				Electrical	Bowlby et al. (1991)
Decapoda	*Acanthephyra purpurea*	3.1×10^{12}	25.2×10^{-9}	490	4	Electrical	Clarke et al. (1962)
Scyphozoa	*Periphylla periphylla*	3.5×10^{10}	0.49×10^{-9}	465	2.4	Electrical	Clarke et al. (1962)
	Atolla wyvillei	1.2×10^{11}	2×10^{-9}	470	2	Mechanical	Nicol (1958)
Siphonophora	*Vogtia glabra*	1.4×10^{11}	1.2×10^{-9}	470	4	Mechanical	Nicol (1958)
	Vogtia spinosa	3.2×10^{11}	1.68×10^{-9}	470	6.5	Mechanical	Nicol (1958)
Pyrosoma	*Pyrosoma atlanticum*	2.3×10^{13}				Mechanical	Bowlby et al. (1990)

photosynthetically available radiant solar energy is at a maximum (Bricaud et al., 2002). At the DYFAMED site in the Ligurian Sea, Sternberg et al. (2007) found downward fluxes of organic matter usually increased in February, were highest in spring and the lowest in autumn but with significant fluxes in June, July and winter in some years. Thus seasonal changes in deep-sea pelagic bioluminescence are likely to occur in the Ligurian Sea but intensity and timing is unpredictable. It might be suggested that by remote sensing of chlorophyll concentrations from satellite sensors and applying appropriate delays it should be possible to forecast bioluminescent activity around a deep-sea telescope array. However, satellite borne ocean colour sensors cannot resolve low chlorophyll concentrations (<0.15 mg m^{-3}) that prevail over large areas of the Mediterranean Sea (Bricaud et al., 2002) so possibilities for reliable prediction seem limited. Short-term changes in bioluminescence may result from spatial patchiness. Heger et al. (2008) discovered a patch of elevated bioluminescence extending down to 1500 m below the surface beneath a mesoscale eddy in the North Atlantic Ocean. In the complex oceanography of the Ligurian Sea (Barth et al., 2005) eddies do occur and may explain the variability in profiles seen in Fig. 3. To take account of all these variations numerous repetitions of the profiles would be required. Submersible observations in the

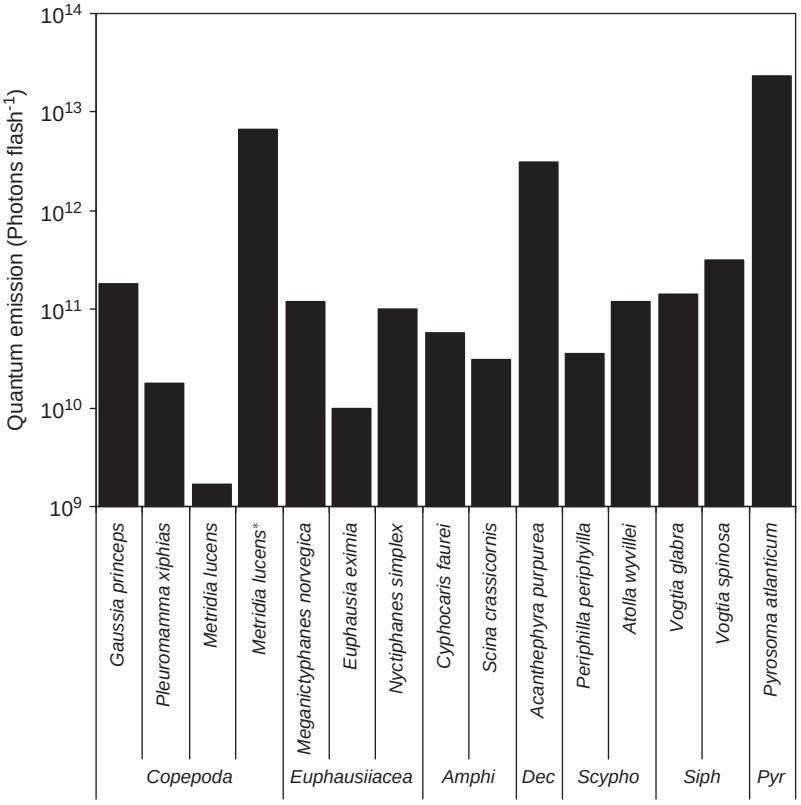

Fig. 4. Estimated quantum emission (photons flash^{-1} into a 4π steradian sphere) for several groups of marine bioluminescent animals. Copepoda, Euphausiiacea, Amphi = Amphipoda, Dec = Decapoda, Scypho = Scyphozoa, Siph = Siphonophora, Pyr = Pyrosoma. Data sources are listed in Table 5. * = Mechanical stimulation of *Metridia lucens*, the other column for this species is electrically stimulated.

Alborán Sea show that incidence of potentially bioluminescent gelatinous plankton such as medusae (24 species), siphonophores (18 species) and ctenophores (22 species) is much higher in the Western Mediterranean than indicated from classical studies on zooplankton distribution in this area (Mills et al., 1996).

The density of bioluminescent organisms in the Ionian Sea at the NESTOR site is extraordinarily low compared with oceanic conditions previously studied. Since the construction of the Aswan High Dam on the river Nile the Eastern Mediterranean basin has been cut off from the main source of surface enrichment with nutrients (Longhurst, 1998) and biological productivity is very low. At depths greater than 2500 m the density of bioluminescent plankton is not significantly different from zero.

The dominant bioluminescent light emission likely to be detected by the underwater telescope is flashes of light resulting from interactions of animals with a photodetector. The predicted background frequency of flashes from interactions between planktonic animals is much lower (Table 4). Buskey and Swift (1990) comment that using dark-adapted human observers in a stationary submersible trimmed to neutral buoyancy such as described by Widder et al. (1989), there was no discernable background bioluminescence even in high abundances of bioluminescent animals. The model of background bioluminescence is highly sensitive to changes in R, the interaction radius, and other assumptions but nevertheless it seems background bioluminescence is small compared with direct interactions with the telescope structure.

The model in Eq. (4) indicates that bioluminescence will be detected by the telescope photon counters as MHz bursts that occur at intervals related to current speed. For ANTARES the prediction of one flash every few minutes seems to be in accord with preliminary data emerging from this experiment (Aguilar et al., 2006). A simple linear relationship is implied between the water current velocity and frequency of bursts. Deviations from such a linear relationship will occur:

(a) During changes in density of organisms as different water masses move past the array.
(b) Changes in frequency of spontaneous or natural bioluminescence deviating from the encounter model in Eq. (5). Animals may vary their flash rates at different times. Priede et al. (2006) speculates that in the Atlantic Ocean if each animal were to flash once per 24 h this could result in a significant background of 30–800 flashes h^{-1} detectable by deep-sea fishes.
(c) As a result of swimming activity of animals which hence impact on detectors independent of current speed.
(d) As a result of entrainment of animals on the array.

(e) Presence of animals capable of emitting a continuous glow rather than solely flashing in response to stimuli (Bowlby et al., 1990; Haddock and Case, 1999).

The intensity of flashes is very difficult to predict with the values in Table 5 giving estimates for fully stimulated organisms. Luminescent animals vary in size from copepods (crustacea) of the order of 1 mm in size to euphausiid shrimps (1–5 cm) to large colonial organisms such as pyrosomes that can grow to over 10 m long and may contain over 100,000 individuals (Priede, personal observation), each capable of multiple flashes. If such an organism became entangled with the array then continuous activity could be anticipated Andersen and Sardou (1994) in a survey of the Mediterranean Sea at depths down to 960 m showed that larger colonies of *Pyrosoma atlanticum* occurred deeper. The smallest organisms are generally the most abundant and we assume that most bioluminescence will be from small crustacea such as copepods. Net sampling to determine species as undertaken by Buskey and Swift (1990) would be very difficult at the deeper depths and lower densities of animals found at the neutrino telescope sites.

Notwithstanding problems of prediction of the actual frequencies and intensities of bioluminescent flashes, the measurement of abundance of sources in the water column provides a firm foundation for investigating relative merits of different sites for construction of neutrino telescopes and understanding variation at those sites. Particularly at the deeper locations in the NESTOR area of the Ionian Sea the bioluminescent flashes are likely to be so rare as to have no influence on performance of a telescope. In this paper we have only considered the direct interactions with the photo-detector sphere, additional light will be emitted from organisms impinging on the adjacent supporting structure. It is evident that the projected area and number of elements of the structure should be minimised. Owing to time delays following stimulation of organisms as they drift past the detector, and presence of down stream entraining vortices it is likely that most bioluminescence will originate from downstream of the photo-detector. In designs where the detector is made up of an assemblage of directional elements this may allow opportunities to filter out biological noise. The KM3NeT observatory infrastructure will also fulfil a function as a long-term environmental observatory (Katz, 2006) and possibilities of using the array to detect bioluminescence background have been discussed. However, Buskey and Swift (1990) comment: "it is not clear that the technical difficulties associated with measuring natural bioluminescence in situ will ever be completely overcome". Most of the bioluminescent signal seen by the neutrino telescope will be artefacts associated with the presence of the telescope structure in a water flow.

Acknowledgements

This work was supported by the EU FP6 KM3NeT Design Study Contract: 011937. J.C. was funded by UK NERC studentship (NE/F012020/1) and A.H. by the Luxembourgish Ministry of Culture. The studies in the Ligurian Sea were financed and supported by the ANTARES collaboration. We thank Professor Andre Freiwald, (University of Erlangen) leader of F.S. *Meteor* cruise M70 leg-1, Spyros Stavrakakis (HCMR) leader of the R.V. *Aegaeo* cruise and colleagues on board these vessels for facilitating work in the Ionian Sea.

References

Aggouras, G., Anassontzis, E.G., Ball, A.E., Bourlis, G., Chinowsky, W., Fahrun, E., Grammatikakis, G., Green, C., Grieder, P., Katrivanos, P., Koske, P., Leisos, A., Markopoulos, E., Minkowsky, P., Nygren, D., Papageorgiou, K., Przybylski, G., Resvanis, L.K., Siotis, I., Sopher, J., Staveris-Polikalas, A., Tsagli, V., Tsirigotis, A., Zhukov, V.A., The NESTOR Collaboration, 2005a. A measurement of the cosmic-ray muon flux with a module of the NESTOR neutrino telescope. Astroparticle Physics 23, 377–392.

Aggouras, G., Anassontzis, E.G., Ball, A.E., Bourlis, G., Chinowsky, W., Fahrun, E., Grammatikakis, G., Green, C., Grieder, P., Katrivanos, P., Koske, P., Leisos, A., Ludvig, J., Markopoulos, E., Minkowsky, P., Nygren, D., Papageorgiou, K., Przybylski, G., Resvanis, L.K., Siotis, I., Sopher, J., Staveris-Polikalas, A., Tsagli, V., Tsirigotis, A., Zhukov, V.A., The NESTOR Collaboration, 2005b. Operation and performance of the NESTOR test detector. Nuclear Instruments and Methods in Physics Research A 552, 420–439.

Aguilar, J., The ANTARES Collaboration, et al., 2006. First results of the Instrumentation Line for the deep-sea ANTARES neutrino telescope. Astroparticle Physics 26 (4–5), 314–324.

Anassontzis, E.G., Koske, P., 2003. Deep-sea station connected by cable to the shore. Sea Technology 44 (7), 10–14.

Andersen, V., Sardou, J., 1994. *Pyrosoma atlanticum* (Tunicata, Thaliacea): diel vertical migration and vertical distribution as a function of colony size. Journal of Plankton Research 16 (4), 337–349.

Babson, J., Barish, B., Becker-Szendy, R., Bradner, H., Cady, R., Clem, J., Dye, S.T., Gaidos, J., Gorham, P., Grieder, P.K.F., Jaworski, M., Kitamura, T., Kropp, W., Learned, J.G., Matsuno, S., March, R., Mitsui, K., O'Connor, D., Ohashi, Y., Okada, A., Peterson, V., Price, L., Reines, F., Roberts, A., Roos, C., Sobel, H., Stenger, V.J., Webster, M., Wilson, C., 1990. Cosmic-ray muons in the deep ocean. Physical Review D 42 (11), 3613–3620.

Barth, A., Alvera-Azcárate, A., Rixen, M., Beckers, J.-M., 2005. Two-way nested model of mesoscale circulation features in the Ligurian Sea. Progress in Oceanography 66, 171–189.

Bowlby, M.R., Case, J.F., 1991. Flash kinetics and spatial patterns of bioluminescence in the copepod *Gaussia princeps*. Marine Biology 100, 329–336.

Bowlby, M.R., Widder, E.A., Case, J.F., 1990. Flash kinetics and spatial patterns of bioluminescence in two pyrosomes. Biological Bulletin 179, 340–350.

Bowlby, M.R., Widder, E.A., Case, J.F., 1991. Disparate forms of bioluminescence from the amphipods *Cyphocaris faurei*, *Scina crassicornis* and *S. borealis*. Journal of Marine Biology 108, 247–253.

Bradner, H., Bartlett, M., Blackinton, G., Clem, J., Karl, D., Learned, J., Lewitus, A., Matsuno, S., O'Connor, D., Peatman, W., Reichle, M., Roos, C., Waters, J., Webster, M., Yarbrough, M., 1987. Bioluminescence profile in the deep Pacific Ocean. Deep-Sea Research 34, 1831–1840.

Bricaud, A., Bosc, E., Antoine, D., 2002. Algal biomass and sea surface temperatures in the Mediterranean Basin. Intercomparison of data from various satellite sensors, and implications for primary productions estimates. Remote Sensing of Environment 81, 163–178.

Buskey, E.J., Swift, E., 1990. An encounter model to predict natural planktonic bioluminescence. Limnology and Oceanography 25 (7), 1469–1485.

Carr, J., Hallewell, G., 2004. Neutrino telescopes in the Mediterranean Sea. New Journal of Physics 6, 112–142.

Clarke, G.L., Conover, R.J., David, C.N., Nicol, J.A.C., 1962. Comparative studies of bioluminescence in copepods and other pelagic animals. Journal of Marine Biological Association of the UK 42, 541–564.

Dussart, B.H., 1965. Les différentes catégories de plancton. Hydrobiologia 26, 72–74.

Gillibrand, E.J.V., Jamieson, A.J., Bagley, P.M., Zuur, A.F., Priede, I.G., 2007. Seasonal development of a deep pelagic bioluminescent layer in the temperate Northeast Atlantic Ocean. Marine Ecology Progress Series 341, 37–44.

Haddock, S.H.D., Case, J.F., 1999. Bioluminescence spectra of shallow and deep-sea gelatinous zooplankton: ctenophores, medusae and siphonophores. Marine Biology 133, 571–582.

Hartline, D.K., Buskey, E.J., Lenz, P.H., 1999. Rapid jumps and bioluminescence elicited by controlled hydrodynamic stimuli in a mesopelagic copepod, *Pleuromamma xiphius*. Biological Bulletin 197, 132–143.

Heger, A., 2007. *In situ* observations of benthic and pelagic bioluminescence in the deep Atlantic Ocean and Mediterranean Sea. Ph.D. Thesis, University of Aberdeen, 188pp.+appendices.

Heger, A., Ieno, E.N., King, N.J., Morris, K.J., Bagley, P.M., Priede, I.G., 2008. Deep-sea pelagic bioluminescence over the Mid-Atlantic Ridge. Deep-Sea Research II 55, 126–136.

Katz, U.F., 2006. KM3NeT: towards a km^3 Mediterranean neutrino telescope. Nuclear Instruments and Methods in Physics Research A 567, 457–461.

Lampitt, R.S., Bett, B.J., Kiriakoulakis, K., Popova, E.E., Ragueneau, O., Vangriesheim, A., Wolff, G.A., 2001. Material supply to the abyssal seafloor in the Northeast Atlantic. Progress in Oceanography 50, 27–63.

Lapota, D., Losee, J.R., 1984. Observations of bioluminescence in marine plankton from the Sea of Cortez. Journal of Experimental Marine Biology and Ecology 77, 209–240.

Latz, M.I., Bowlby, M.R., Case, J.F., 1990. Recovery and stimulation of copepod bioluminescence. Journal of Experimental Marine Biology and Ecology 136, 1–22.

Longhurst, A., 1998. Ecological Geography of the Sea. Academic Press, San Diego, USA, 398pp.

Margiotta, A., On behalf of the NEMO Collaboration, 2006. Status report of the NEMO (Neutrino Mediterranean Observatory) project. Physica Scripta 127T, 107–108.

Mills, C.E., Pugh, P.R., Harbison, G.R., Haddock, S.H.D., 1996. Medusae, siphonophores and ctenophores of the Alborán Sea, south western Mediterranean. Scientia Marina 60, 145–163.

Nicol, J.A.C., 1958. Observations on luminescence in pelagic animals. Journal of the Marine Biological Association of the United Kingdom 37, 705–752.

Priede, I.G., Bagley, P.M., Way, S., Herring, P.J., Partridge, J.C., 2006. Bioluminescence in the deep-sea: free-fall lander observations in the Atlantic Ocean off Cape Verde. Deep-Sea Research I 53, 1272–1283.

Sieburth, J.McN., Smetacek, V., Lenz, J., 1978. Pelagic ecosystem structure: heterotrophic compartments of the plankton and their relationship to plankton size fractions. Limnology and Oceanography 23, 1256–1263.

Sternberg, E., Jeandel, C., Miquel, J.-C., Gasser, B., Souhaut, M., Arraes-Mescoff, R., Francois, R., 2007. Particulate barium fluxes and export production in the northwestern Mediterranean. Marine Chemistry 105, 281–295.

Stolarczyk, T., ANTARES Collaboration, 2007. ANTARES first muons with the first line. Nuclear Physics B (Proceedings Supplement) 165, 188–195.

Webster, M.S., Roos, C.E., Roberts, A., Okada, A., Ohashi, Y., O'Connor, D., Mitiguy, R., Matsuno, S., March, R., Learned, J.G., Karl, D., Clem, J., Blackinton, G., Bradner, H., Babson, J., 1991. Mechanical stimulation of bioluminescence in the deep Pacific Ocean. Deep-Sea Research 38, 201–217.

Widder, E.A., Bernstein, S.A., Bracher, D.F., Case, J.F., Reisenbichler, K.R., Torres, J.J., Robison, B.H., 1989. Bioluminescence in the Monterey submarine canyon—image-analysis of video recordings from a midwater submersible. Marine Biology 100, 541–551.

Widder, E.A., Johnsen, S., Bernstein, S.A., Case, J.F., Neilson, D.J., 1999. Thin layers of bioluminescent copepods found at density discontinuities in the water column. Marine Biology 134, 429–437.

Wood, S.N., 2006. Generalised Additive Models. An Introduction with R. Chapman & Hall/CRC, Boca Raton, FL.

Zuur, A.F., Ieno, E.N., Smith, G.M., 2007. Analysing Ecological Data. Springer, New York, 672pp.